

Planar Serial Manipulator Motion Synthesis

Yanhui Wei^{*}, Han Han, Zepeng Wang, Xin Liu and Guangchun Li

(College of Automation, Harbin Engineering University, Harbin 150001, China)

Abstract: This paper deals with the universal serial manipulator on the inverse kinematics problem of plane type, the fast working space solution method, and the obstacle avoidance path planning method. With the vector projection as the main constraint condition of the target, it proposes a general form of the inverse kinematics solution which does not depend on the robot configuration of freedom degree. By identifying the target vector direction maximum and minimum workspace boundary and determining the destination vector by thick search on the workspace boundary method, an expressing method of the polar coordinate form of work space is then introduced. Finally, according to the form of plane trajectory planning for obstacle avoidance problem, the method of solving the inverse kinematics solution of the concave and convex forms of the safe obstacle avoidance area is improved. The simulation results verify that the proposed method has feasibility and generality.

Keywords: planar serial manipulators; inverse kinematics; workspace; trajectory planning; vector projection

CLC number: TP391.7

Document code: A

Article ID: 1005-9113(2015)02-0049-07

1 Introduction

Planar serial manipulators refer to the feature in which a robot can point in a two-dimensional plane movement at the end of a series. Planar serial robot motion control is easy to implement, in which a robot forms a single, large range of movement of each joint. Considerable classic serial robot configuration has evolved. For example, PUMA robot increases the first rotary joints to the second and third joints based on planar configuration and satisfies the requirement of a three-dimensional space robot position by orthogonal layout to request the position of space operating point. Planar serial manipulators have been advanced in some special circumstances, such as under water-type robot arm.

For the space robot kinematics analysis, the robot configuration can be divided into multiple planar configuration forms. Reconfigurable robot through a module can free the combination of complex robot configuration and address the kinematics analysis, dynamics analysis, and trajectory planning problems. To solve the inverse kinematics solution of an automatically reconfigurable robot, Wei et al.^[1] proposed the concept of configuration plane. In this concept, a three-dimensional robot configuration is

decomposed into a two-dimensional plane configuration to simplify the inverse kinematics problem and achieve the goal of an automatic and fast solution. Generally, the analytic solutions are difficult to obtain due to the multi-parameters, nonlinearity and coupling of the solutions, and the algebra equations involved in the inverse kinematics of 6R serial manipulators^[2]. Wei et al.^[3] used a semi-analytic method and a general method to solve the spatial n R robot inverse kinematics problem. A motion analysis has been conducted with any form of planar configuration, which becomes a reconfigurable robot series and is one of the key problems of the robot motion analysis.

In this paper, the inverse kinematics of planar serial manipulators and the workspace and trajectory planning are studied, with the vector projection method as the focus. This study aims to obtain a simple and fast method and a general inverse kinematics solution for the reconfigurable robot trajectory planning and to provide a reference for space in the form of serial manipulators.

2 Automatic Kinematics Solution

2.1 General Form of Planar Serial Manipulators

Planar serial manipulators are mainly composed of rotational joints, translational joint, and a connecting

Received 2013-12-04.

Sponsored by the National Natural Science Foundation of China (Grant No. 51205074), the Specialized Research Fund for the Doctoral Program of Higher Education (Grant No. 20112304120007), the Harbin Specialized Research Foundation for Innovation Talents (Grant No. RC2012QN009037), the Fundamental Research Funds for the Central Universities (Grant No. HEUCF041505), and the State Commission of Science Technology of China (Grant No. 2014DFR10010).

^{*} Corresponding author. E-mail. wyhhit@163.com.

rod. Considering that the connecting rod is not in the form of a single connection, when a robot motion model is established, with the rotational joint of the basic movement unit, the motion transformation matrix is

$$T = \begin{bmatrix} \cos \theta & -\sin \theta & h \cos \theta \\ \sin \theta & \cos \theta & h \sin \theta \\ 0 & 0 & 1 \end{bmatrix} \quad (1)$$

where θ is the rotational joint exercise; h is the length of the connecting rod of two adjacent rotational joint centers, whose value varies when it includes mobile joints.

The general form of planar serial manipulators is shown in Fig.1. The end point of the pose matrix is:

$$T = T_1 T_2 \cdots T_n = \begin{bmatrix} \cos(\theta_1 + \cdots \theta_n) & -\sin(\theta_1 + \cdots \theta_n) & a \\ \sin(\theta_1 + \cdots \theta_n) & \cos(\theta_1 + \cdots \theta_n) & b \\ 0 & 0 & 1 \end{bmatrix} \quad (2)$$

where

$$\begin{aligned} a &= h_n \cos(\theta_1 + \cdots \theta_n) + \cdots h_2 \cos(\theta_1 + \theta_2) + h_1 \cos(\theta_1) \\ b &= h_n \sin(\theta_1 + \cdots \theta_n) + \cdots h_2 \sin(\theta_1 + \theta_2) + h_1 \sin(\theta_1). \end{aligned}$$

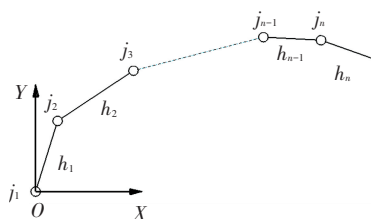


Fig.1 General form of the planar serial manipulator motion model

2.2 Automatic Solving Method of Planar Serial Manipulator

This method does not contain considerable translational joint in a common conformation of planar serial manipulator but meets the space position requirements or space redundant tasks. The excessive movement of the robot joints will reduce the performance and stiffness characteristics in the overall controlling process.

As shown in Fig.1, the inverse kinematics of planar serial manipulator can be divided into two parts, i.e., the posture and position requirements. For the planar serial robot with a redundant form (more than three degrees of freedom), their posture requirements are under the conditions that the first $n - 1$ joint part must guarantee the range of n joints' motion. The end posture requirements can be achieved through the last one rotating joints, and its location requirements can be implemented by combining the first $n - 1$ joints. For the planar serial robot whose degree of freedom is less

than or equal to 3, its three joints all need to meet the posture and position requirements and it can be analytically solved using Eq.(2). We use the vector projection method to solve the various forms of planar serial robot automatically, which satisfies the following constraints:

$$\|p\| = \sum_{i=0}^n a_i h_i \quad (3)$$

where $\|p\|$ is the norm of the end vector; a_i is the ratio between the projection of i th joint lever arm on the vector \vec{p} and the joint lever arm. Considering the direction of vector projection, a_i is expressed as follows:

$$a_i = h_i \cos(\theta'_i) \quad (4)$$

where θ'_i is the angle between i th joint lever arm and the target point vector.

In Fig.2, P point is the target point. If the length h_n of the joint n is fixed, the spatial location of the joint's sports center can be calculated. Therefore, the entire calculation is after a combination of the former $N - 1$ joint, and the ends of the joint $n - 1$ coincide with the center joint n in the figure. Without a fixed length, mobile joints exist, which utilize the shortest length. The joint I to the joint $n + 1$ between the lever arm is in a state of maximum length, ensuring that the length of $j_{i+1}j_n$ is maximum. The center of the joints with the picture n is calculated, which is the tentative for j'_n .

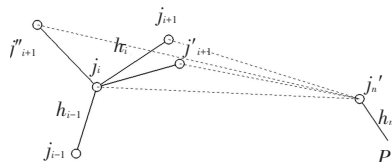


Fig.2 Kinematics solving process

The automatic calculation is elucidated as follows:

(1) In the case of joint movement i range, the projection quantity maximum.

Point (j'_{i+1}) of j_{i+1} is found in $j_j j'_n$, as shown in Fig.2. The length of $j'_{i+1} j_n$ is compared with that of $j'_{i+1} j'_n$; if $j'_{i+1} j'_n > j'_{i+1} j_n$, $i + 1$ joint automatic calculation is conducted; if $j'_{i+1} j'_n \leq j'_{i+1} j_n$, the next step is performed;

(2) In the case of joint movement i range, the inverse projection quantity.

Maximum point (j''_{i+1}) of j_{i+1} is found in $j_j j'_n$, as shown in Fig.2. The length of $j''_{i+1} j_n$ is compared with that of $j''_{i+1} j'_n$; if $j''_{i+1} j'_n \geq j''_{i+1} j_n$, the automatic calculation is conducted at the end of I joint. In the case of joint movement I range, $j_{i+1} j'_n$ is found to meet the requirements; otherwise, the next step is

performed;

(3) $I + 1$ joint is adjusted to $n - 1$ joint exercise to make the length of $j''_{i+1}j_n$ be the shortest. The length of $j''_{i+1}j_n$ is compared with that of $j''_{i+1}j'_n$; if $j''_{i+1}j'_n \geq j''_{i+1}j_n$, the length of $j''_{i+1}j_n$ is adjusted to meet the position requirements; if $j''_{i+1}j'_n < j''_{i+1}j_n$, the inverse projection quantity maximum point of j_jj_{i+1} is found in $j_jj'_n$ and $I + 1$ joint automatic calculation is conducted.

Starting from the first joint, a constant cycle can meet the requirements at the end of the robot kinematics inverse solutions.

2.3 Simulation Instance

For building a five degree-of-freedom planar robot configuration, the length of each link is shown in Table 1. The configuration of the target formation, as shown in Fig.3, is $j_1j'_2j'_3j'_4j'_5P$.

Table 1 Link parameters and range of motion

h_1 (cm)	h_2 (cm)	h_3 (cm)	h_4 (cm)	h_5 (cm)
50	40	30	10	5
$\theta_1(^{\circ})$	$\theta_2(^{\circ})$	$\theta_3(^{\circ})$	$\theta_4(^{\circ})$	$\theta_5(^{\circ})$
± 70	± 90	± 60	± 100	± 90

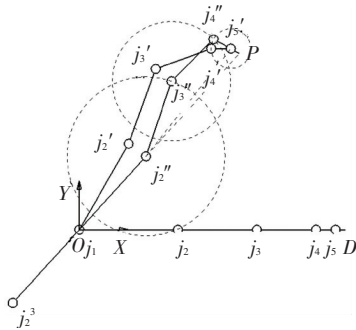


Fig.3 Solving process diagram

The target matrix is as follows:

$$T = \begin{bmatrix} 0.866 & 0.500 & 81.201 & 7 \\ -0.500 & 0.866 & 88.649 & 6 \\ 0 & 0 & 1.000 & 0 \end{bmatrix} \quad (5)$$

The solving process is as follows:

1) As shown in Fig.3, the initial configuration of the robot is $j_1j_2j_3j_4j_5$. According to the automatic solution process, we make joint 5 meet the posture requirements of robots. Through the inverse solution, the spatial location of joint 5's rotating center - j'_5 is calculated. In the range of motion of joint 1, the point of j''_2 is found, ensuring that $j_1j''_2$ in the projection of Oj'_5 is the largest. The comparison of the length of j_2D with that of $j''_2j'_5$ indicates that $j_2D > j''_2j'_5$;

2) In the motion range of joint 1, the point of j_2^3 is found, ensuring that $j_1j_2^3$ in the inverse projection of Oj'_5 is the largest. The comparison of the length of j_2D with

that of $j_2^3j'_5$ indicates that $j_2D < j_2^3j'_5$. Owing to the limit of the motion range of joint 2, the joint length between joint 2 and the end of the robot in the actual formation is significantly less than j_2D , which we can achieve by adjusting the amount of exercise from joints 2 to 5.

3) A circle is drawn with the center j''_2 and the radius j_2j_3 , i.e., Round 1. Another circle is drawn with the center j'_5 and the radius j_5j_4 , i.e., Round 2. The point between Rounds 1 and 2 is j''_3 . Another circle is drawn with the center j''_3 and the radius j_3j_4 , i.e., Round 3. The intersection between Rounds 2 and 3 is j''_4 . If $\angle j''_2j'_3j'_4$, $\angle j'_3j''_4j'_5$, and $\angle j''_4j'_5P$ meet the range of motion of joints 3, 4, and 5, respectively, the calculation is correct; otherwise, we should re-adjust the position of j''_3 .

After the above steps, we can obtain the solution of inverse kinematics, as shown in Table 2.

Table 2 Solution of inverse kinematics ($^{\circ}$)

θ_1	θ_2	θ_3	θ_4	θ_5
47.51	23.56	-46.29	-72.82	-1.97

3 Automatic Solution of the Workspace

3.1 Description of the Problem

The workspace of the robot, which can show the operating range that the robot can achieve, is an important indicator for evaluating robots. However, the workspace of planar robot differs because the number of composition joint and the range of motion also differ. Thus, the workspace we obtain is complex and will form a complex region, which is made of multi-domains, as shown in Fig. 4. This feature makes the solution of the workspace difficult to obtain.

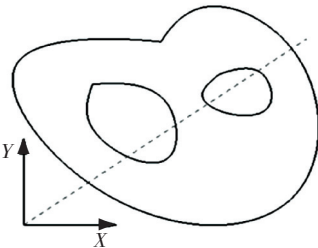


Fig.4 Workspace made of multi-domains

The method for solving the robot workspace mainly includes analytical, graphical, and numerical methods^[4]. In the analytical method, the boundary of workspace is determined by multiple envelopes. However, this method is complicated and is generally applied to the robots with less than three joints^[5]. The graphical method is used to solve the boundary of workspace. We can obtain various intersecting lines or intersecting surfaces. This method is effective but is

also limited by the number of degrees of freedom. When the number of joints is large, we should handle it by group^[6]. The numerical method is based on extreme value theory and optimization methods to calculate the feature points on the boundary surfaces of robots' workspace, which are used to constitute the boundary curves and form the boundary surface. The representative results are the search method, iterative method, and Monte Carlo^[7-9]. In order to compute the constant-orientation workspace of serial robots, a fast search method based on the binary approximating principle is proposed^[10].

Based on the above methods, each method aims to utilize the area formed by the workspace. The problem of automatically solving the workspace is the determination of the boundary of the workspace. As shown in Fig. 4, to facilitate the rapid evaluation workspace of planar serial manipulator and the fast matching configuration plane of reconfigurable robots, we usually give plane vector to solve the position that the robot can achieve on the vector. In this paper, we use a method based on the workspace expression of planar serial manipulator in the polar form, i.e., in the condition in which the space vector is known, the workspace boundaries on this vector angle is rapidly determined.

3.2 Auto-solving Methods

1) Solving the maximum polar angle in the target vector direction.

When the polar angle of the target vector is in the motion range of the first swing module, its maximum is

$$H_{\max} = \sum_{i=1}^n H_{i\max} \quad (6)$$

When the polar angle of the target vector is not in the motion range of the first swing module, as shown in Fig. 5; a is the maximum limit of the first swing module, and b is the vector angle of the target vector, and $j_2 j_n$ is the maximum length of other joints; the first joint is placed on the limit angle that is nearest to the polar angle, and the second swing joint is placed on the limit angle which is the same as the first one. The position coordinates of j'_n is solved. We then observe whether its polar angle and the limit angle of the first swing joint are distributed on each side of the vector of the target polar coordinates. If they do not distribute on each side of the vector of the target polar coordinates, we continue to find all joints in the same way. If all the swing joints are found, we are still not able to distribute the polar angle of j'_n with the limit angle of the previous swing joint on the both sides of the target vector angle; therefore, the end of the planar configuration cannot reach the target point in this vector angle. If a swing joint is in the limit angle, the polar angle of j'_n is distributed with the limit angle of the

previous swing joint on the both sides of the target vector angle. The configuration plane can then achieve the maximum distance value in the polar coordinate corner of the target vector.

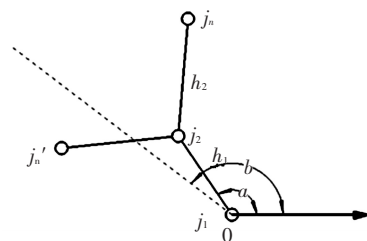


Fig.5 Schematic of solving the maximum

2) Solving the minimum polar angle in the target vector direction.

Solving the minimum value of the polar angle is complex. If the maximum value exists, the minimum will also exist.

A swing center is firstly found in the configuration plane. The lengths of two parts, which are divided by the swing center in the configuration plane, must have the smallest difference, as shown in Fig.6. The centers of the swing module, which are O_2 and O_3 , are placed at the limit area. We observe whether they interfere to the non-biased swing module, as shown in Fig. 6, whose cross will not cause in its configuration plane.

In $\Delta O_1 O_2 O_3$, we can obtain the result of $O_2 O_3$, as well as $\angle O_1 O_2 O_3$ and $\angle O_1 O_3 O_2$.

a) $\angle O_1 O_2 O_3$ and $\angle O_1 O_3 O_2$ are in the limit of the swing joints, of which at this time $O_2 O_4$ and $O_3 O_5$ interfere; thus, the minimum value is zero.

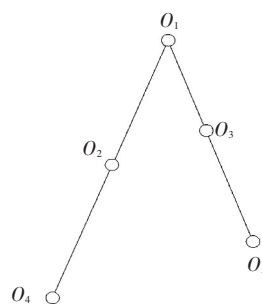


Fig.6 Schematic of the determination of the swing center of the configuration plane

b) $\angle O_1 O_2 O_3$ or $\angle O_1 O_3 O_2$ is out of the limit of the swing joints. Supposing $\angle O_1 O_3 O_2$ is out of the limit, as shown in Fig.7, $\angle O_1 O_3 O_5$ is the limit angle. If $O_3 O_5$ has a swing joint, we can consider the swing joint closest to O_3 as the center, i.e., O'_3 . We rotate the module to coincide the line $O'_3 O_5$ with the vector $O'_3 O_2$. The distance of $O_2 O_5$ is calculated, and the lengths $O_2 O_5$ and $O_2 O_4$ are determined. If $O_2 O_5 \leq O_2 O_4$, the minimum value in the polar angle is zero;

otherwise, O_2O_4 will rotate to the vector line O_2O_5 , and O_4O_5 is the minimum value in the polar angle.

c) $\angle O_1O_2O_3$ and $\angle O_1O_3O_2$ are beyond the limit of swing joint. These two joints are placed at the limit position. With the same case solving process, the minimum value of O_4O_5 can be easily found.

3) Searching the interval boundaries in the target vector direction.

The interval boundaries for the multi-connected region boundary are searched in the target vector direction.

Considering the balance between accuracy and speed, two search methods, namely coarse and fine search methods of combining, are used.

a) Coarse search. Coarse search is used to determine the approximate area of the space boundary and utilizes an equal interval to research. The search range is the known polar angle. The target vector direction maximum and minimum methods are used for solving $[l_{\min}, l_{\max}]$ area. The previously described solving planar serial manipulator methods are then used to judge whether the achieved plane point is in the robot workspace.

b) Fine search. Refined search is through the space boundaries determined by coarse search. The boundary point that satisfies certain precision is searched. The dichotomy method is used to determine more accurate multi-connected region boundary.

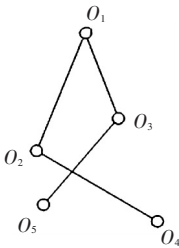


Fig.7 Schematic of the minimum solution

4 Trajectory Planning Method

4.1 Problem Description

The objective of trajectory planning is to plan ideal task and joint space trajectories, make the robot motion fast, accurate and stable with high movement point efficiency and high trajectory tracking accuracy, and satisfy the path, obstacle, and kinematics constraints.

The obstacle avoidance is a key problem in the trajectory planning. The usual approach used is planning the robot end-point space trajectory, meeting the space avoiding obstacle requirements, and using robot inverse kinematics to solve each joint value at each space point. Adjusting the speed and acceleration of the translational joint allows the robot to achieve

better motion effects. To achieve the obstacle avoidance task better, many studies have simplified the barriers' outline by enveloping circle^[11]. In Ref. [12], the barrier approximates a point and takes the minimum distance between the point and the lever arm as the basis of obstacle avoidance. This method expands the obstacle space, reduces the actual robot working space in the actual working environment, and limits the robot's workability. Xie et al.^[13] used new bi-directional rapidly exploring random tree algorithms for complex spatial obstacle avoidance trajectory planning. These algorithms do not require the inverse kinematics calculation method, but we can achieve the spatial obstacle avoidance task by expanding the tree method.

Duguleana^[14] proposes a new approach for solving the problem of obstacle avoidance during manipulation tasks performed by redundant manipulators. In which q-learning is used together with neural networks in order to plan and execute arm movements at each time instant.

Perumaal et al.^[15] proposed an automated trajectory planner to determine a smooth, minimum-time and collision-free trajectory for the pick-and-place operations of a 6-DOF robotic manipulator in the presence of an obstacle. The proposed planner is able to handle the trajectory with and without via-point and traces the smooth, collision-free, near-time-optimal trajectory. The collision-free trajectory is ensured not only for the robot's end-effector but also for its links.

Capisani et al.^[16] proposed a simple but effective path planning strategy. The goal is to represent the obstacles in the robot configuration space. The representation allows obtaining an efficient and accurate trajectory planning and tracking. And a dedicated collision checking rule between the manipulator and obstacles is also proposed.

Section 2 describes the method for solving the robot kinematics. When space obstacles exist, their spatial trajectory is planned. Interference will occur with the obstacle, as shown in Fig.8.

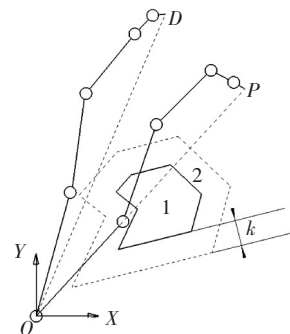


Fig.8 Planar configuration inverse movement solving the obstacle avoidance problem

We continue to use the simulation example of

Section 2, in which the robot moves from the initial point D to the target point P . The area 1 in Fig.8 is formed by the actual obstacle. Considering the robot link's dimension and safe distance, we expand zone 1 in k distance, which forms the secure avoiding obstacle zone 2. According to the inverse kinematics solution during the trajectory planning, the final form of the robot configuration shows noticeable interference. How to balance the inverse kinematics automatic solution and the obstacle avoidance is to be solved.

4.2 Method of Improving Trajectory Planning

The planar serial manipulator automated solution process remains unchanged. The results must be preprocessed to satisfy the conditions for joint constraint under spatial avoidance issues. The solution process is as follows.

1) Interference judgment of the obstacle area.

Obstacle avoidance safety zone is a closed planar region and is an irregular region that can be represented by multiple segments connected orderly on its border. Planar robot is composed of multistage lines that are connected. We can determine whether interference exists between the robot and the obstacle region based on whether the boundary line of the safe obstacle avoidance area intersects with the topological structure line of the robot.

The security avoidance zone is set consisting of m line segments. i line segment can be expressed as

$$y = \frac{(y_i - y_{i-1})(x - x_{i-1})}{x_i - x_{i-1}} + y_{i-1} \quad (7)$$

The robot configuration consists of n period of line segments. Therefore, j th line segment is represented by the following equation:

$$y = \frac{(y_j - y_{j-1})(x - x_{j-1})}{x_j - x_{j-1}} + y_{j-1} \quad (8)$$

Two lines exist in plane geometry, either parallel or intersecting. To improve the efficiency of the judgmental process, we firstly compare Eq.(7) with Eq.(8) and judge whether the slope of the two segments are equal; if not, we solve the two intersecting straight lines and then judge whether the intersection point between the two lines is equal.

The robot chassis and ends cannot be in the obstacle region according to the robot features. Otherwise, the robot is unable to complete the work. Therefore, obstacle interference exists, i. e., the boundary line of the safe obstacle avoidance area and the topological structure line of the robot present interference. Judging all robot joints and the segments among the security barrier regions is not necessary to improve the overall efficiency of the robot planning calculation. In accordance with the method of planar robot inverse kinematics solution in Section 2, we only judge the first part of the robot joints and the boundary

line near the robot base side in the security barrier region. Once the obstruction interference situations occur, we should repeat the trajectory planning.

2) Improvement and simulation of space obstacle avoidance trajectory planning.

When obstacles exist in the robot working area, we should guide the end of the robot joints to the target point approximation beginning with joint 1, with Eq.(3) as constraint. Meanwhile, we should conduct an interference checking to plan the joint in the obstacle areas and lead the robot to avoid the obstacle joint area.

Fig.9 shows the simulation example. The path of the end point is planned with the interpolation method, which reveals that the method has a good effect on individual concave and convex obstacle areas and its computational efficiency is more rapid than using A * algorithm, as shown in Fig.9.

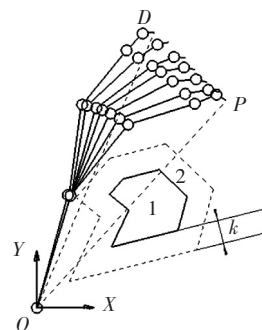


Fig.9 Trajectory planning simulation

Some concave area cannot meet the target location or satisfy the target position, as shown in Fig. 10, where 1 is the safe obstacle avoidance concave area. This figure shows the obstacle avoidance method of robot configuration. A great distance exists between the robot end and the target point.

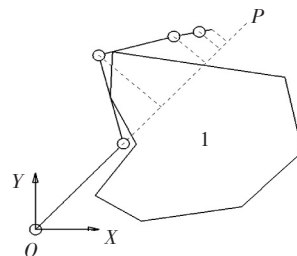


Fig.10 Concave obstacle area of the obstacle avoidance simulation example

As joints 1 and 2 approach to the target and obstacle avoidance areas in the robot configuration in Fig.10, the robot joints on the target vector projection cannot meet the requirement of Eq.(3). Joints 1 and 2 have a compensatory ability of target point space vector projection by rotating. We may easily obtain the target

point space vector difference of the robot's configuration by calculating Δ . Then, we have

$$\Delta = \|p\| - \sum_{i=1}^n a_i h_i. \quad (9)$$

To meet the requirements of the robot end-point stance, the final robot joint lever arm at the end of the vector projection is fixed. The change parameters are the target point of the projection ratio for $n-1$ knuckle arm. Eq.(9) is modified as follows:

$$\Delta = \|p\| - \sum_{i=1}^{n-1} a_i h_i - a_n h_n. \quad (10)$$

The requirements of obstacle avoidance and joint angle constraint should be satisfied, and the first $n-1$ joints should be turned, and the projection value of the lever arm at each robot joint on the target point vector must be increased on the basis of the robot configuration. The values of the projection sizes can be obtained by calculating Eq.(4).

The robot configuration is shown in Fig.11.

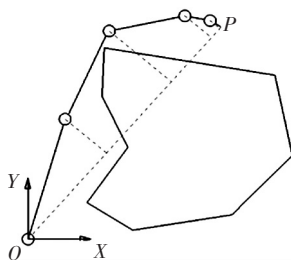


Fig.11 Simulation after the trajectory planning method is improved

5 Conclusions

1) Using the constraints of the vector projection method and joints, the kinematics problem of the planar serial manipulator is solved. The simulation results show that this method avoids the traditional analytical method which relies on the forms of robot configurations and the degrees of freedom, as well as the problem of solving speed and precision when using numerical methods. This method is also practical and versatile.

2) A working range is proposed in the direction of the vector as the workspace expression of planar robot. This method uses a searching way to solve the workspace range rapidly in the direction of the setting vector angle. This method is also automatic and fast. Furthermore, this method is the foundation of the research in decomposing a three-dimensional space robot into a two-dimensional planar robot.

3) Through the inverse kinematics solution method of planar serial manipulator with improved forms, the trajectory plan is achieved when the workspace of a planar robot presents obstacles. The simulation results show that the method is versatile and practical to the barrier with a convex form.

References

- [1] Wei Yanhui, Zhao Jie, Gao Yanbin, et al. The study on a kinematics solving method for reconfigurable modular robots. *Journal of Harbin Institute of Technology*, 2010, 42 (1): 133-137. (in Chinese)
- [2] Liu Y J, Huang T. Inverse kinematics and trajectory planning of 6R serial manipulators. *Journal of Mechanical Engineering*, 2012, 48 (3): 9-15. (in Chinese)
- [3] Wei Yanhui, Jian Shengqi, He Shuang, et al. General approach for inverse kinematics of nR robots. *Mechanism and Machine Theory*, 2014, 75: 97-106.
- [4] Cui Yujie, Li Zhangzu, Fan Lei. Based on Monte Carlo methods picking manipulator workspace analysis. *Agricultural Mechanization Research*, 2007, 12: 62-64. (in Chinese)
- [5] Xu W F, Li L T, Liang B, et al. Workspace analysis of space 3R robot. *Journal of Astronautics*, 2007, 28 (5): 1389-1394. (in Chinese)
- [6] Guo Li, Gao Wenjie. Sanitary ceramics glazing robot workspace Research. *Machine Tool & Hydraulics*, 2007, 35(6): 29-32. (in Chinese)
- [7] Diao X M, Ou M. Workspace analysis of a 6-DOF cable robot for hardware-in-the-loop dynamic simulation. *Proceedings of the 2006 IEEE/RSJ International Conference on Intelligent Robots and Systems*. Beijing, 2006. 4103-4108.
- [8] Piao M B. Research on workspace of a two-arm surgical robot. *Proceedings of the 2007 IEEE International Conference on Mechatronics and Automation*. Harbin, 2007. 1067-1072.
- [9] Zhao Jie, Wang Weizhong, Cai Hegao. Algorithms for automatically determining workspace of reconfigurable robots. *Journal of Tianjin University*, 2006, 39(9): 1082-1087. (in Chinese)
- [10] Zhu Haifei, Guan Yisheng, Wu Wenqiang. A fast search method for computing the constant-orientation workspace based on the binary approximating principle. *Robot*, 2013, 35(6): 709-715. (in Chinese)
- [11] Jia Qingxuan, Chen Gang, Sun Hanxu, et al. Path planning for space manipulator to avoid obstacle based on A* algorithm. *Journal of Mechanical Engineering*, 2010, 46 (13): 109-116. (in Chinese)
- [12] Fang Cheng, Zhao Jing. New dynamic obstacle avoidance algorithm with hybrid index based on gradient projection method. *Journal of Mechanical Engineering*, 2010, 46 (19): 29-37. (in Chinese)
- [13] Xie Biyun, Zhao Jing, Liu Yu. Motion planning of reaching point movements for 7R robotic manipulators in obstacle environment based on rapidly-exploring random tree algorithm. *Journal of Mechanical Engineering*, 2012, 48 (3): 63-70.
- [14] Duguleana M, Barbuceanu F G, Teirlebar A, et al. Obstacle avoidance of redundant manipulators using neural networks based reinforcement learning. *Robotics and Computer-Integrated Manufacturing*, 2012, 28(2): 132-146.
- [15] Perumaal S S, Jawahar N. Automated trajectory planner of industrial robot for pick-and-place task. *International Journal of Advanced Robotic Systems*, 2013, 10: 1-17.
- [16] Capisani L M, Facchinetti T, Ferrara A, et al. Obstacle modelling oriented to safe motion planning and control for planar rigid robot manipulators. *Journal of Intelligent & Robotic Systems*, 2013, 71(2): 159-178.